128 SHADES OF RED: Objective Remote Assessment of Radiation Dermatitis by Augmented Digital Skin Imaging

Richard PARTL[a,1], Beata JONKO[b], Stefan SCHNIDAR[b], Michael SCHÖLLHAMMER[b], Max BAUER[b], Sanchit SINGH[b], Julia SIMECKOVA[b], Kathrin WIESNER[b], Andreas NEUBAUER[c], Harald SCHNIDAR[b]

[a]*Medical University of Graz - Department of Therapeutic Radiology and Oncology, Graz, Austria*
[b]*SCARLETRED Holding GmbH, Vienna, Austria*
[c]*Apeiron Biologics AG, Vienna, Austria*

Abstract. The purpose of our investigation was to develop a novel and state of the art digital skin imaging method capable for remote monitoring and objective assessment of Radiation Induced Dermatitis (RID). Therefore, radiation therapy related side effects were assessed by medical experts according to Common Terminology Criteria for Adverse Events (CTCAE) grade of severity in 20 female breast cancer patients in a clinical trial over the treatment time frame of 25-28 radiation cycles, 50.0 – 50.4 Gy each. Furthermore the intensity of developed skin erythema was documented by using conventional spectrophotometry plus digital skin imaging. Thereby we could derive the Standardized Erythema Value (SEV), a novel objective parameter, which in contrast to single parametric L* and a* delivers a long dynamic measurement range for analyzing RID from bright to very dark skin tones. Methodical superiority of the SEV could be proven over spectrophotometer measurements in terms of a higher sensitivity and by enabling signal intensity mapping in analyzed skin images. Our thereupon-derived patent enables novel objective dermatologic eHealth applications in a broad range of medical and industrial use by opening likewise the window for augmented dermatology. The first of its kind system is now already further developed in form of the medical device product Scarletred®Vision. It is available on the market for primary usage in clinical trials and in medical routine.

Keywords. Radiation Dermatitis, Standardized Erythema Value (SEV), Skin Erythema, eHealth, Augmented Dermatology, Scarletred®Vision

1. Introduction

The purpose of the investigation was to develop a novel and state of the art digital skin imaging method capable for remote monitoring and objective assessment of radiation induced dermatitis (RID) for usage in clinical trials and medical routine. Radiation damage of the skin can occur as a result of cancer treatment and represents one of the most frequent side effects of radiotherapy leading to acute inflammation in 95% of patients, whereof in 87% of patients moderate to severe RID occurs during or at the end of the treatment [1]. The pathophysiological cause for the reaction is linked to massive radical oxygen species (ROS) production, which is induced during irradiation treatment

---

[1] Corresponding Author: Dr. med. Richard PARTL, Address: Medical University of Graz - Department of Therapeutic Radiology and Oncology, 8036 Graz, Austria, E-Mail: richard.partl@medunigraz.at.

and in the course of radiochemotherapy [2, 3]. The frequency as well as the severity of the reaction depends on aspects associated with the therapy (radiation quality, dose per fraction, cumulative dose, fraction scheme, size of the treatment area, concomitant therapy, previous radiation, localization of irradiated area) and on aspects associated with the patient (skin type, sensitivity to radiation, concomitant diseases) ranging from moderate erythema to deep ulcerations. Pruritus, erythema, skin distension, epitheliolysis, and pain affect not only the quality of life but also pose a risk of an infection of open wounds. Consequently, this may lead to treatment interruptions or discontinuations of the irradiation therapy and longer deferment of the subsequently planned system therapy. Although there is still no evidence that prophylactic treatments, beyond keeping the irradiated area clean and dry, are effective in reducing the incidence or severity of RID [4], most physicians advocate the topical use of aloe vera gel, trolamine, or Aquaphor (a petrolatum-based ointment) to minimize discomfort [5, 6]. However promising novel therapeutic concepts in the treatment of inflammatory conditions rooted in the neutralization of increased ROS levels are in advanced clinical research (ClinialTrials.gov identifier NCT01513278). Treatment associated toxicities can impair quality of life and adversely affect outcome. In order to cope with these dermal toxicities a sensitive and early detection, precise documentation and objective classification are of great importance.

Current state of the art to classify these skin reactions is based on the visual inspection of morphologic alterations only. The most common system is the Common Terminology Criteria for Adverse Effects (CTCAE v. 4.03), developed by the Radiation Therapy Oncology Group (RTOG) and the National Cancer Institute (NCI), dividing skin reactions into five distinct grades, according to the degree of severity [7]. Grade 1 changes include faint erythema or dry desquamation, which may be accompanied by pruritus, skin distension, hair loss, and pigment alteration. These changes normally occur a couple of days or up to a couple of weeks after the beginning of treatment. Grade 2 RID changes include moderate to brisk erythema or a patchy moist desquamation, mostly confined to skin folds and creases, and a moderate edema. These changes are often painful and bear an increased risk of infection [8]. In grade 3 RID the area of moist desquamation spreads to areas outside of the skin folds. Hemorrhage from minor trauma and abrasion are often present. Grade 4 RID is a life-threatening condition characterized by skin necrosis and ulceration of full thickness dermis. There is a particularly high risk of spontaneous bleeding. These changes are very painful and are characterized by poor healing. Skin grafts may be needed. Grade 5 RID leads to the death of the patient. The shortcomings of this, and also other clinical classification systems is mainly based on the subjective assessment and thus on the description of the observed skin condition, whose perception can vary greatly among assessors and may even differ in one assessor in the course of one day. A further drawback of this method is the classification in only five grades. Thus minor differences in the skin condition, as needed for clinical evaluation and comparison of the effectiveness of topical medication, cannot be sufficiently indicated, especially when study groups are small. For reduction of inter- and intra-observer variability as well as for early, sensitive and quantitative assessment of the degree of RID, objective tools are urgently needed.

Method establishment was carried out in the course of a Phase I drug trial (NCT01513278) wherein 20 female patients with histologically confirmed early-stage breast cancer were included to prove safety/efficacy of a novel biological medical product in the treatment of RID. In parallel to this we conducted 2862 single point spectrophotometric measurements, each consisting of three specific color coordinates

(L*a*b*) within the CIELAB color space [9]. At this initial basis we could derive the SEV, a novel objective parameter which is capable of measuring erythema based skin alterations by simultaneously providing a long dynamic range from bright to very dark skin tones (Fitzpatrick Type 0 to 5). In contrast to spectrophotometric methods measuring L*, a* or b* only, the SEV is based on the algorithm $(L*_{max} - L*) \times a*$. It can be used independently of the skin type, and takes into account the basic or even a changing skin color of a subject. The observed change in the analyzed erythema signal was shown to be statistically significant higher ($p<0.0001$) with our algorithm when compared to single parametric measurement of a*, proving the higher sensitivity of our method. We consequently applied the SEV method on taken digital skin images, whereby to our surprise for the first time erythema waves could be unveiled reflecting the applied irradiation treatment setup. Due to this we assume that our derived novel skin imaging and analysis method is superior to spectrophotometry. It is assumed being capable to measure both, the efficacy and side effects of investigational novel skin drugs and treatment methods for RID and any other related inflammatory skin diseases.

2. Methods

2.1. Study design

In the period between February and June 2012, 20 female patients with histologically confirmed early-stage breast cancer, who underwent prior breast-conserving surgery, were included in a prospective clinical study (ClinialTrials.gov identifier, NCT01513278). Further eligibility requirements were: Age 18 years or older, Karnofsky Performance Status (KPS) ≥ 80% and Bra cup size ≤ D. Patients were excluded if they had bilateral or inflammatory breast cancer, lymphangiosis carcinomatosa, medically significant dermatologic conditions affecting the irradiated area, if the use of other agents with the aim of preventing and/or treating RID was planned, if they took concomitant medications which might exacerbate radiation damage on the skin, and had a history of previous breast radiation therapy.

2.2. Radiotherapy setup

All patients received whole-breast irradiation by using the Clinac® iX system linear accelerator (Varian Medical Systems Inc.) and applying standard opposed medial and lateral tangent fields to a total dose of 50.0 – 50.4 Gy in 25 – 28 fractions (5 x 1.8 – 2 Gy/week). Dosimetric measurement was done via thermoluminiscent diodes (TLD) to validate the locally applied dose at the skin surface. According to the study protocol, RID was assessed daily, based on the EORTC/RTOG-CTCAE v4.03 classification system beginning at baseline before the start of radiotherapy.

2.3. Data acquisition by Spectrophotometry

Spectrophotometric skin measurement was carried out at screening and daily from fraction 6 to fraction 25/28 always prior to the application of the study medication. The Spectrophotometer CM-700d (Konica Minolta, Tokyo, Japan) was used with a measurement diaphragm Ø 8mm in MAV and auto-calibration mode. Data of six single

spot measurements was collected per investigation time point and patient in determined areas of the medial/lateral breast region. In total 2862 measurements were carried out, each comprising the complete L*a*b* (CIELAB) color space, a global used industry standard approved by the French Commission Internationale de l'Èclairage (CIE) [9]. It describes all the colors visible to the human eye and was created to serve as a device-independent model to be used as a reference. The three coordinates of the CIELAB reflect the values of a measured color with respect to the lightness (**L***, ranging from black to white), its position on the red/green axis (**a***, negative values indicate green while positive values indicate red) and its position on the yellow/blue axis (**b***, negative values indicate blue and positive values indicate yellow). For objective analysis we separated the parameters L*, a* and b* for each individual patient (#01 to #20) and mean values were calculated per fraction (FR01 to FR28) and region.

2.4. Data acquisition by Digital Color Imaging

In parallel to spectrophotometry, 1431 digital photographs of the irradiated areas were taken with the Canon Digital Cam G12 (Canon Inc., Tokyo, Japan) under stable light conditions, standardized device settings and by co-imaging the prototype of the Scarletred® color reference marker (SCARLETRED Holding GmbH, Vienna, Austria). A representative subset of the images from patients with either developed grade 0, grade 1 or grade 2, was used to prove the applicability of the derived SEV method.

2.5. Color space conversion

To calculate the SEV, we convert the image from the RGB into the CIELAB color space in two steps, starting with the linear transformation of the RGB to CIEXYZ [10] (Eq. 1):

$$\begin{pmatrix} X \\ Y \\ Z \end{pmatrix} = M_{RGB}^{-1} * \begin{pmatrix} R \\ G \\ B \end{pmatrix} \tag{1}$$

$$with \quad M_{RGB}^{-1} = \begin{pmatrix} 0.412453 & 0.357580 & 0.180423 \\ 0.212671 & 0.715160 & 0.072169 \\ 0.019334 & 0.119193 & 0.950227 \end{pmatrix}$$

ISO13655 [11] includes the current specification of the CIEXYZ to CIELAB conversion as follows (Equation 2):

$$L^* = 116 * Y' - 16 \qquad a^* = 500 * (X' - Y') \qquad b^* = 200 * (Y' - Z') \tag{2}$$
$$C_{ref} = (X_{ref}, Y_{ref}, Z_{ref})$$

with

$$X' = f_1\left(\frac{X}{X_{ref}}\right), Y' = f_1\left(\frac{Y}{Y_{ref}}\right), Z' = f_1\left(\frac{Z}{Z_{ref}}\right)$$

$$f_1(c) = \begin{cases} c^{\frac{1}{3}} & for\ c > \epsilon \\ \kappa * c + \dfrac{16}{116} & for\ c \le \epsilon \end{cases}$$

where

$$\epsilon = \left(\frac{6}{29}\right)^3 = \frac{216}{24389} \qquad \qquad \kappa = \frac{1}{116}\left(\frac{29}{3}\right)^3 = \frac{841}{108}$$

C_{ref} is the reference white point of a specified illuminant. We use the D65 (indirect daylight) with C_{ref} = (0.95047, 1.0, 1.08883) illuminant as a reference.

2.6. In Silico Image Analysis

A redness gradient was generated starting from the darkest red color to the brightest red color by in silico method using a color depth of 8 bit per color channel R'G'B'. This was achieved by increasing the value of the primary R' in the R'G'B' (RGB) color space from 0 to 255 (8 bit) and then kept constant. On the increasing side of R', the primaries G' and B' were set constant to the value 0 whereas on the constant side of R', both G' and B' start from 0 and increase to 255 in a step size of 1. The resulting values were converted into the CIELAB color space. Corresponding erythema values were calculated by the formula ((255 – L*) × a*), divided by 255 to get comparable values in the range from 0 to 255. For obtaining only the red contingent of the CIELAB color space, signal cut off for a* was defined at 128. For objective quantitative assessment and comparison between single images, gained erythema signals were normalized in the range 0-1 and optionally also used for signal intensity mapping in a next step [12].

2.7. SEV Signal Intensity Mapping

The calculated SEV signal was extracted from the original image as a grey value image. Subsequently the high dynamic SEV grey scale images were pseudo colored to optimize for human perception. Each single intensity value was mapped to a color according to our developed SEV color map, which is designed and tailored to the underlying signal. It defines a color gradient over the minimum to maximum signal range enabling to visualize more details and potential signal saturation [12].

2.8. Statistical Data Analysis

Data was summarized with respect to demographic and baseline characteristics, safety observations and measurements, and efficacy observations and measurements. Summary statistics include the mean, N, standard deviation, median, quartiles, minimum, and maximum values for continuous variables, and frequencies and percentages for categorical variables. Demographics and baseline data was summarized overall by using standard summary statistics. For all variables assessed, conducted statistical tests (paired t-testing, unpaired t-testing) and estimated p-values are descriptive.

3. Results

Patient demographics: All patients were Caucasian female with a median age of 58 years (range, 40-72). In 10 patients the carcinoma was located in the right breast, in 10 in the left breast. The most common skin type according to the Fitzpatrick scale was skin type 3 (65%), followed by skin type 2 in 20% of the population. One patient had diabetes mellitus type 2 and another one had a contact dermatitis to band-aids. One patient discontinued the participation in the study, thus the analyzed population included 19 patients (n = 19). Overall, the incidence of RID grade 2 was low. Only 4 out of 20 patients (20%) developed grade 2 RID, whereas 14 developed grade 1 RID (70%). Only

Table 1. Patient characteristics (n=20 patients)

Characteristics	mean / median	n / %
Age in years	57.8 / 58.9	
TNM classification		
pTis		03 / 15
pT1mi		01 / 05
pT1a		02 / 10
pT1b		04 / 20
pT1c		09 / 45
pT2		01 / 05
Body mass index (mean / median)	28.1 / 27.5	
Bra cup size		
A		02 / 10
B		07 / 35
C		09 / 45
D		02 / 10
Radiation field size per treatment side (cm^2)	236.4 / 229.0	
Skin Type (Fitzpatrick scale)		
1		01 / 05
2		04 / 20
3		13 / 65
4		02 / 10
CTCAE grade of the RID (0 - 4)		
0		01 / 05
1		14 / 70
2		04 / 20
n.d. (withdrawn from the study)		01 / 05

one patient (#18) did not develop signs of radiation skin damage. One patient has withdrawn the participation from the study after the first week of cancer irradiation treatment (Table 1).

3.1. Negative correlation between L* and a*

Spectrophotometric data analysis delivered longitudinal alterations of L* and a* values by a statistical significant decrease of mean L* (p=0.0002) and a significant increase of mean a* values (p<0.0001) over irradiation time, which is in alignment with the literature [13, 14, 15]. No statistical significance was observed for the b* value (p=0.4357). A negative correlation between both objective parameters can be shown by calculating the slope (m) for L* (m=-0.1589) and a* (m=0.137) over time (Figure 1A). Patients with RID grade 2 (n=5) delivered a significant lower mean L* (60.04) when compared to patients with RID grade 1 (64.48, p<0.0001). Unpaired t-testing of a* between RID grade 2 (10.5) and 1 (8.08) reached also statistical significance (p<0.0001) (Figure 1B).
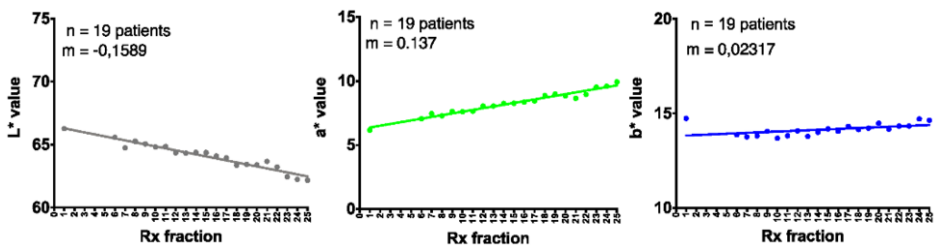

Figure 1A. Signal trend analysis of spectrophotometry data and paired t-testing of baseline versus irradiation fraction 25 for L* (p < 0.0002, ***), a* (p < 0.0001, ****) and b* (p = 0.4357); n = 19, m = slope
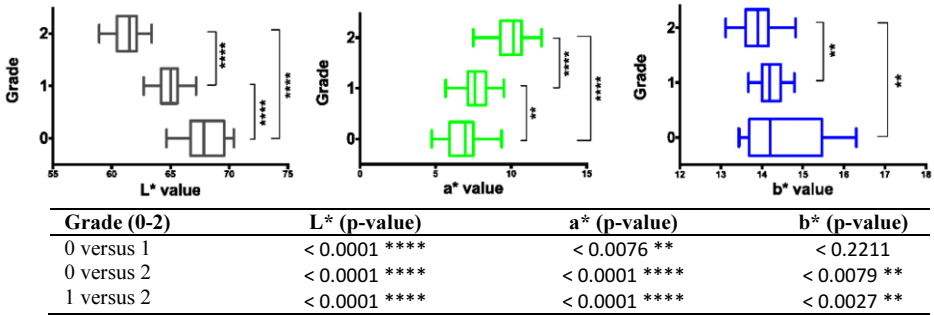
Grade (0-2)	L* (p-value)	a* (p-value)	b* (p-value)
0 versus 1	< 0.0001 ****	< 0.0076 **	< 0.2211
0 versus 2	< 0.0001 ****	< 0.0001 ****	< 0.0079 **
1 versus 2	< 0.0001 ****	< 0.0001 ****	< 0.0027 **

Figure 1B. Unpaired t-testing of single spectrophotometric parameter L*, a* and b* with developed RID grading 0-2; n = 19

3.2. Novel erythema parameter with superior sensitivity

To make synergistic use of the opposing tendency of a* and L*, we combined the parameters by developing the algorithm $(L*_{max} - L*) \times a*$, gaining the Standardized Erythema Value (SEV). The calculated increase of the SEV over time delivered a high statistical significance (p<0.0001, m=6,797) (Figure 2A). Unpaired t-testing of the SEV shows a significant correlation with the developed RID between grading 1 and 2 (p<0.0001; n=19). Furthermore the SEV shows a higher relative fold increase (2.02-fold) over treatment time when compared to the single parameter a* (1.61-fold). Despite of the fact that in most patients the developed erythema was rather faint and RID grade 2 was only observed in 21% of the patients, the change in the erythema signal between gained min/max values was significantly higher (p<0.0001) for the SEV when compared to a*. The superiority of the SEV for measuring erythema can thus be proven (Figure 2B).

3.3. Higher dynamic application range of the SEV*

In-Silico analysis of the measured a* values revealed a significant decrease with higher skin darkening, which consequently leads to a* value duplicates on the gained erythema signal intensity curve. Such a* values, however, may reflect either light or dark red, leading to the problem that gained a* values cannot be discriminated clearly from each other and over a certain investigation time, which represents a major pitfall of the spectrophotometric method. In contrast, our developed SEV formula overcomes this methodical weakness by delivering a higher dynamic application range of the measured erythema signal when compared to the single parameter a* (Figure 3).
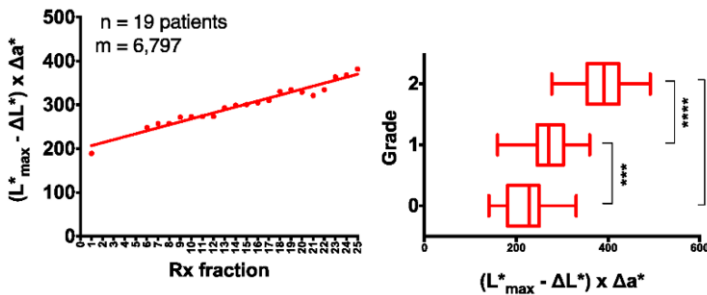

Figure 2A. Signal trend analysis of spectrophotometry data and unpaired t-testing of the SEV given by $(L*_{max} - L*) \times a*$ with developed RID grading; m = slope
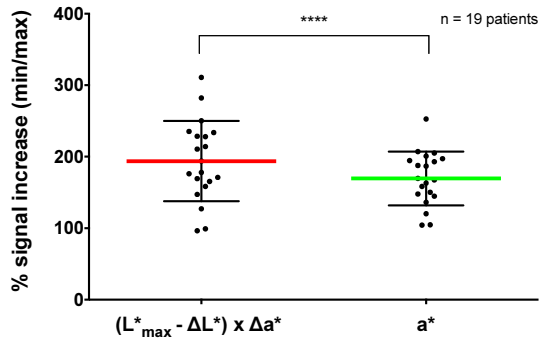
Figure 2B. Superior sensitivity of the SEV for measuring changes in the intensity of erythema when compared to a* (p<0.0001); shown mean and SD of spectrophotometry

3.4. High-density image data analysis reveals cycling erythema waves

The application of the SEV method on taken patient images delivered longitudinal alterations of the SEV mean signal over irradiation time, reflecting also the outcome of spectrophotometry. Also fitting to this result, unpaired t-testing of the measured SEV signals delivered a high statistical significance between the clinically assessed RID grade 0 and 2 (p<0.0001) and RID grade 1 and 2 (p<0.0005). In contrast to spectrophotometric analysis of the SEV, no statistical significance could be detected via image analysis between RID 0 and 1 (Figure 4).

Most surprisingly pronounced cycling waves of the measured SEV signal could be detected via image analysis on the single patient level. The detected erythema waves align well to the weekly irradiation cycle. The highest slope for the measured erythema could be observed in the patient #11 (m = 0.00196), which by clinical assessment developed only a RID grade 1, reflecting a SEV of 0.066 at the end of the investigation period. In comparison to this, patient #18 finished the study with a RID grade 0 (m=0.00067, SEV 0.049) (Figure 5).
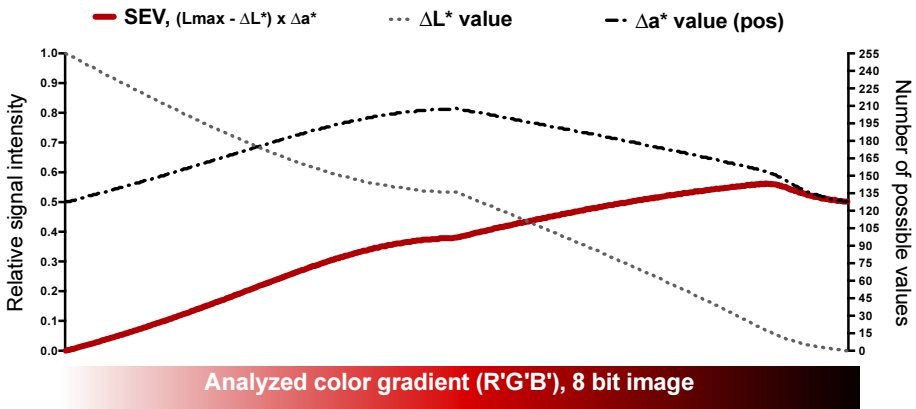

Figure 3. In silico image analysis of a created erythema gradient; Calculated SEV, L* and a* values are based on 8 bit per channel according to the CIE L*a*b* color space
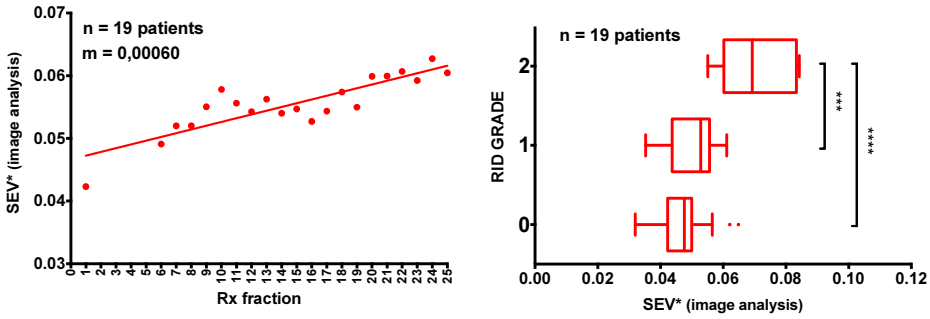
Figure 4. Objective image analysis of the developed skin erythema over study time and unpaired t-testing of the SEV* with developed RID grading; n=19 patients, m = slope

3.5. Augmented Dermatology

Pseudo-signal mapping of the measured SEV signal was carried out for the time points present on the trend line to visualize the signal trend and assumed heterogeneous appearance of the developed skin erythema, which was existent in most of the patients. Patient #11 developed the highest slope of the SEV over treatment time and is thus given as a representative example in the augmented visualization of the developed SEV signal (Figure 6).

4. Discussion

Despite of the fact that nowadays numerous mobile digital devices can support clinicians already by efficient local data collection, signal tracking and objective remote analysis, a convenient and efficient solution for objective measurement of visual skin changes is still pending. Thus the aim of this paper was to identify visual objective parameters to create a novel method enabling efficient, automated and remote assessment of erythema related skin diseases such as the radiation induced dermatitis (RID) in clinical practice
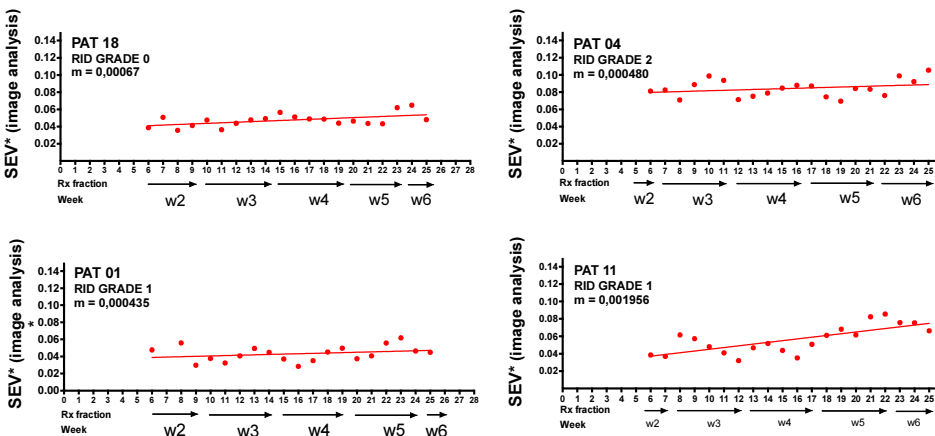

Figure 5. Cycling erythema waves: Objective image analysis of the developed skin erythema (SEV) in individual patients over treatment time; w = week
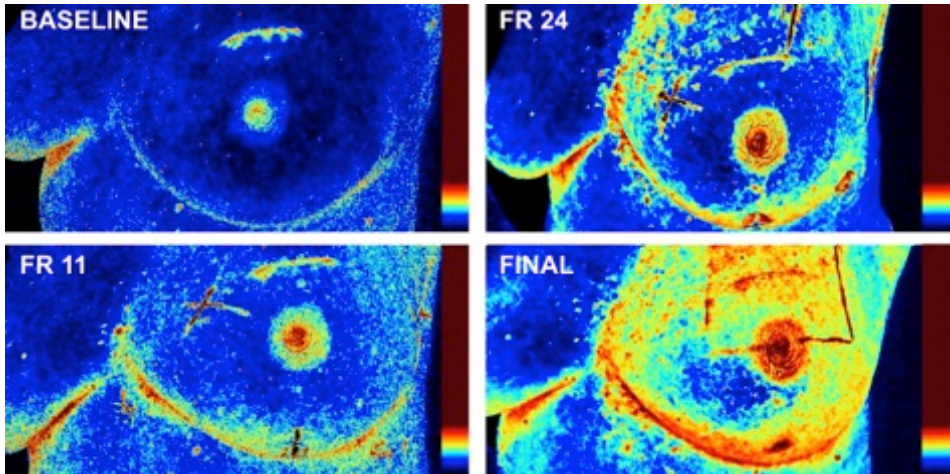
Figure 6. Augmented Dermatology by pseudo-color signal intensity mapping of the SEV; exemplary images of patient #11 at baseline, FR 11, FR 24 and study end (final)

and trials. According to historical data, breast size, smoking history, body mass index (BMI) and comorbidities such as diabetes, rheumatoid arthritis and hypertension are under suspicion to be correlated with an increased risk for the development of RID in the course of cancer irradiation therapy [3]. However the currently published data is conflicting and reliable prognostic parameters are still missing. According to a recent single blind randomized phase III trial in breast cancer patients, no association between dermatitis and BMI or breast size were observed [4], which is in line with our own observations (Table 1).

As a basis for our study, time resolved spectrophotometric analysis was conducted to quantify the intensity of erythema in combination with clinical assessment of observed skin toxicities in 20 irradiated female breast cancer patients. We observed RID grade 0-2 varying from mild erythema to moist desquamation confined to the breast fold. The radiation field size (cm^2) and the Fitzpatrick-Scale (1-2 vs. 3-4) did not deliver a statistical significant correlation with RID grade 2 in our trial. According to previous studies spectrophotometric measurement of a* and L* values are still suggested as objective parameters useful for analyzing RID [13-15]. In contrast to this we could prove that assessment of a* alone fails completely due to the possible generation of a* value duplicates, which impedes its usage for objective quantitative erythema assessment. As shown by In-Silico analysis the observed effect is caused by a significant decrease of the measured a* signal when simultaneously lowering the L* (Figure 3). In a biological context, a decrease in the L* value can simply be caused by an increase in skin pigmentation, which is typically observed in the development of RID. This means, the higher a*, the more intense is the skin reddening and the lower L* the more pigmented becomes the patient`s skin upon irradiation treatment (Figure 1 A/B). Due to this measured a* value duplicates can either originate from a light or a dark red skin region, which thus cannot be quantitatively distinguished by current spectrophotometric methods. Fitting to this result the a* value alone provides a linear scaling of the measured signal only for a very narrow application range, when hemoglobin or melanin content in the skin are low [14, 15]. Consequently in a clinical study a higher hemoglobin or

melanin content can lead the investigator to an over- or underestimation of the visually perceived skin reddening and hence connected skin toxicities.

Our novel method however overcomes the pitfall of spectrophotometric skin analysis by introducing the Standardized Erythema Value; SEV (Figure 2 A/B). Importantly and in strict contrast to methods which apply the L*, a* or b* value only, the SEV enables objective quantification of skin erythema (Figure 4). It can be used in a broad range of skin types, and considers the basic or even a changing skin color of a subject over investigation time. Thereby it is the first objective erythema parameter, which provides a linear scale from bright skin (Fitzpatrick skin type I) to very dark skin tones (Fitzpatrick skin type VI) [12]. This can be essential not only in context of RID but also in other skin diseases where visual skin color changes are evident.

To our surprise, application of the SEV method on consecutively taken patient images could also increases the quality of erythema assessment in such a magnitude that for the first time cycling erythema waves became visible on a single patient level. The pronounced erythema waves are well synchronized with the weekly irradiation treatment, which includes two days of treatment pause over the weekend (Figure 5). Such significant higher resolution of the image analysis results from the high data density of a pixel by pixel based quantification of the SEV signal, which in contrast to the spectrophotometric analysis is by a magnitude of $1x10^6$ higher, due to the high number of available measurement replicates. Thereby the superiority of the SEV for usage in image analysis can be proven over spectrophotometry, especially when visual differences in the erythema are low or the signal appears inhomogeneous and the selection of representative skin areas is difficult for the individual observer. A more detailed follow up investigations on the single patient level leads us now also to assume that a higher SEV at baseline might be associated with an increased risk to develop RID grade 2 and higher. Whether the SEV can prospectively also serve as a novel risk parameter for developing severe forms of RID need to be still proven in a bigger patient cohort, which upon success could consequently enable an early therapeutic intervention and/or fine tuning of the currently used standard irradiation treatment setup.

Furthermore by combining the method with the potential of signal intensity mapping we could open a window to Augmented Dermatology (Figure 6). The powerful tool is assumed being capable to prospectively support the objective assessment of skin erythema and time dependent visual changes of skin inflammation or pigmentation not only in RID but as well in any other inflammatory skin reaction where objective assessment of the erythema intensity and scoring of the erythema over time is of relevance, such as in contact dermatitis, rosacea, acne, psoriasis, erysipelas, chronic wounds, systemic lupus, Kawasaki disease and drug allergy, only to provide some representative examples.

Due to the broad medical application scope of our technology we have patented and developed the method already further in form of the CE marked medical device product Scarletred®Vision. The first of its kind medical device platform is fully mobile and capable to run on commercial smartphones. It also integrates a novel digital Gold Standard in form of a skin patch, which serves as an internal reference and enables to standardize and automate the process of image documentation and measurement by computational assisted analysis of taken skin images with respect to varying local light conditions and the distance of the imaged object. The dermatologic eHealth technology is in use in a broad range of medical and industrial applications and supplied online via www.scarletredvision.com.

Ethical conduct of the study

The study was carried out in accordance with the Declaration of Helsinki, all applicable laws and regulations of Austria, where the study was conducted, and in compliance with the current Good Clinical Practice guideline (CPMP/ICH/135/95). It was approved by the appropriate IEC and by the Austrian competent authority AGES (Österreichische Agentur für Gesundheit und Ernährungssicherheit).

References

[1]   McQuestion M; Evidence-based skin care management in radiation therapy; Semin Oncol Nurs. 2006; 22(3):163-73

[2]   Tanaka E, Yamazaki H, Yoshida K, Takenaka T, Masuda N, Kotsuma T, Yoshioka Y, Inoue T.; Objective and longitudinal assessment of dermatitis after postoperative accelerated partial breast irradiation using high-dose-rate interstitial brachytherapy in patients with breast cancer treated with breast conserving therapy: reduction of moisture deterioration by APBI; Int J Radiat Oncol Biol Phys. 2011 Nov 15; 81(4):1098-104.

[3]   Kasapović J, Pejić S, Stojiljković V, Todorović A, Radošević-Jelić L, Saičić ZS, Pajović SB; Antioxidant status and lipid peroxidation in the blood of breast cancer patients of different ages after chemotherapy with 5-fluorouracil, doxorubicin and cyclophosphamide, Clinical Biochemistry 43 (2010) 1287–1293

[4]   Bolderston A, Lloyd NS, Wong RK, Holden L, Robb-Blenderman L; Supportive Care Guidelines Group of Cancer Care Ontario Program in Evidence-based Care; The prevention and management of acute skin reactions related to radiation therapy: a systematic review and practice guideline; Support Care Cancer (2006) 14: 802–817 DOI 10.1007/s00520-006-0063-4

[5]   Fisher J, Scott C, Stevens R, et al. Randomized phase III study comparing best supportive care to biafine as a prophylactic agent for radiation-induced skin toxicity for women undergoing breast irradiation: Radiation Therapy Oncology Group (RTOG 97-13. Int J Radiat Oncol Biol Phys 2000; 48:1307-1310

[6]   Elliott EA, Wright JR, Swann RS, et al. Phase III Trial of an emulsion containing trolamine for the prevention for the prevention of radiation dermatitis in patients with advanced squamous cell carcinoma of the head and neck: Results of Radiation Therapy Oncology Group Trial 99-13. J Clin Oncol 2006; 24:2092-2097

[7]   Cox. JD, Stetz JA, Pajak TF; Toxicity Criteria of the Radiation Oncology Group and the European Organisation for Research and Treatment of Cancer (EORTC), Int J Radiat Oncol Biol Phys 1995; 31:1341-1346

[8]   Hymes SR, Strom EA and Five C: Radiation dermatitis: clinical presentation, pathophysiology, and treatment 2006; J Am Acad Dermatol. 2006 Jan; 54(1): 28-46

[9]   Commission Internationale de l'Eclairage; Colorimetry, 3rd Edition. Tech. rep. 2004

[10]   Burger W. and Burge M.J.; Digital Image Processing: An algorithmic introduction using java texts in computer science; Springer London, 2016

[11]   Graphic technology – Spectral measurement and colorimetric computation for graphic arts images. Standard. Geneva, CH: International Organization for Standardization, ISO, 2009

[12]   Schnidar H and Neubauer A; Methods for assessing Erythema; European Patent 2976013A1, Jan.2017

[13]   Yoshida K, Yamazaki H, Takenaka T, Tanaka E, Kotsuma T, Fujita Y, Masuda N, Kuriyama K, Yoshida M, Nishimura T; Objective Assessment of Dermatitis Following Post-operative Radiotherapy in Patients with Breast Cancer Treated with Breast-conserving Treatment; Strahlenther Onkol 2010 No 11

[14]   Takiwaki H; Measurement of skin color: practical application and theoretical considerations", The journal of medical investigation; JMI, 1 February 1998 (1998-02-01), page 121

[15]   Chardon A et al. Skin color typology and sun tanning pathways; International Journal of Cosmetics Science, vol. 13, no. 4, 1 August 1991 (1991-08-01), pages 191-208